ACS Macro Letters

pubs.acs.org/macroletters Letter

Nanovaccine Based on Glycocalyx-Mimicking Nanovehicle to Potentiate the Immunogenicity of Neoantigen

Yiwei Shi, Xuyang Xu, Xiaomei Liu, Xin Liang, Xiangyun Xu, Long Li,* and Guosong Chen

Cite This: ACS Macro Lett. 2026, 15, 165−173 Read Online

ACCESS | Metrics & More | Article Recommendations | Supporting Information

ABSTRACT: Neoantigens are promising candidates for personalized cancer vaccines and immunotherapies. However, low immunogenicity and insufficient cross-presentation of neoantigens remain a major challenge. Inspired by natural glycocalyx and its important functions in immune response, here we report a glycocalyx-mimicking nanovehicle constructed from (oligo)mannoside-modified acid-sensitive glycopolymers to improve the efficiency of tumor neoantigens. These amphiphilic glycopolymers assembled into nanoparticles could serve as immune activators for dendritic cells maturation. The encapsulation of neoantigens in the glycopolymer nanocarrier improves the physicochemical properties and endosomal escape of the antigens, thereby not only enhancing their uptake and cross-presentation by dendritic cells but also promoting cytotoxic T cell proliferation and proinflammatory cytokine secretion. These results indicated that the glycocalyx-mimicking nanovehicle integrating delivery and immune adjuvant functions provides a promising platform for cancer vaccines.

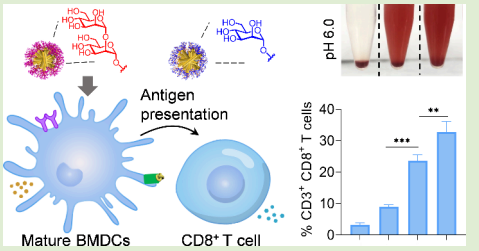

Vaccines, mainly composed of antigens and adjuvants, make important contributions to the prevention and treatment of diseases.[1,2] For tumor treatments, tumor vaccines provide a way to induce autologous antitumor immune responses by stimulating antigen-presenting cells (APCs) and then initiating antigen-specific T cell immunity.[3−5] Traditionally, proteins overexpressed in cancer cells have been widely used as antigens, but their therapeutic efficacy is limited due to central and peripheral immune tolerance.[6,7] With the development of large-scale sequencing, neoantigens have been identified from somatic genetic events that are present only in cancer cells, such as tumor somatic mutations and gene rearrangements.[8,9] They are highly specific in tumor tissues and carry no risk of autoimmune toxicity, offering a promising approach for personalized cancer vaccines and immunotherapy.[10,11] However, as subunit antigens, these neoantigens composed of abundant nonpolar and aliphatic amino acids suffer from insufficient immunogenicity and poor pharmacokinetic properties for vaccine preparation, potentially due to poor solubility and easy aggregation, which limit their internalization by APCs.[12,13] Furthermore, subunit antigens have to effectively escape from endosomes to induce cytotoxic T cell immune responses, which relies on antigen presentation by APCs via the major histocompatibility complex I (MHC I) pathway.[14−16] Thus, it is highly valuable for developing efficient approaches to improve physicochemical properties of neoantigens and enhance the delivery efficacy of neoantigen vaccines.

The glycocalyx is a polysaccharide layer on the cell membrane that could selectively interact with carbohydrate recognition proteins of immune cells to influence immune activation, regulation, and evasion.[17−20] Driven by the indispensable functions of the natural glycocalyx, synthetic glycopolymers have been engineered as multivalent scaffolds for novel biomaterials, offering advantages such as high-density saccharide presentation, facile chemical modification, tunable self-assembly into nanostructures, and excellent biocompatibility.[21−28] Beyond their physicochemical attributes, the glycopolymers could also engage immune cell carbohydrate recognition receptors to direct extracellular biosignaling, showing potential for immune applications.[29,30] However, the potential of glycopolymers as adjuvants remains underexplored, partly because the multistep synthesis of carbohydrates cannot be easily integrated with controlled polymerization methods. Here, we report a glycopolymer-based nanocarrier with inherent immune-activating capabilities that enhance the immunogenicity of neoantigens (Scheme 1). The amphiphilic glycopolymers were constructed by grafting mannopyranoside (Man) or dimannopyranoside (*d*Man) onto a block copolymer, and formed nanoparticles in aqueous solution. These glyconanoparticles significantly induced the proinflammatory activity and maturation of bone marrow-derived dendritic cells (BMDCs), which are usually stimulated by potent adjuvants.[31−35] Taking advantage of this bioactivity, the neoantigen

Received: October 24, 2025
Revised: December 24, 2025
Accepted: January 2, 2026
Published: January 9, 2026

https://doi.org/10.1021/acsmacrolett.5c00712
ACS Macro Lett. 2026, 15, 165−173

Scheme 1. Schematic Illustration of the Glycocalyx-Inspired Nanovaccine Enhancing Neoantigen Immunogenicity via Improved Endocytosis and Cross-Presentation by APCs

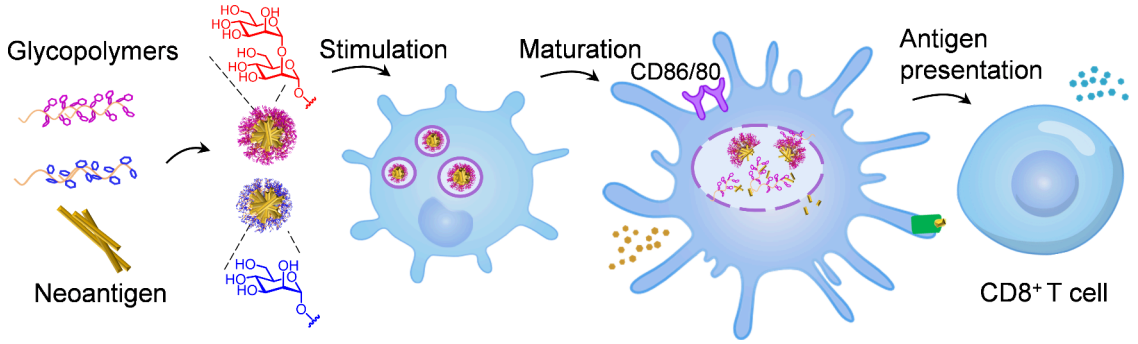

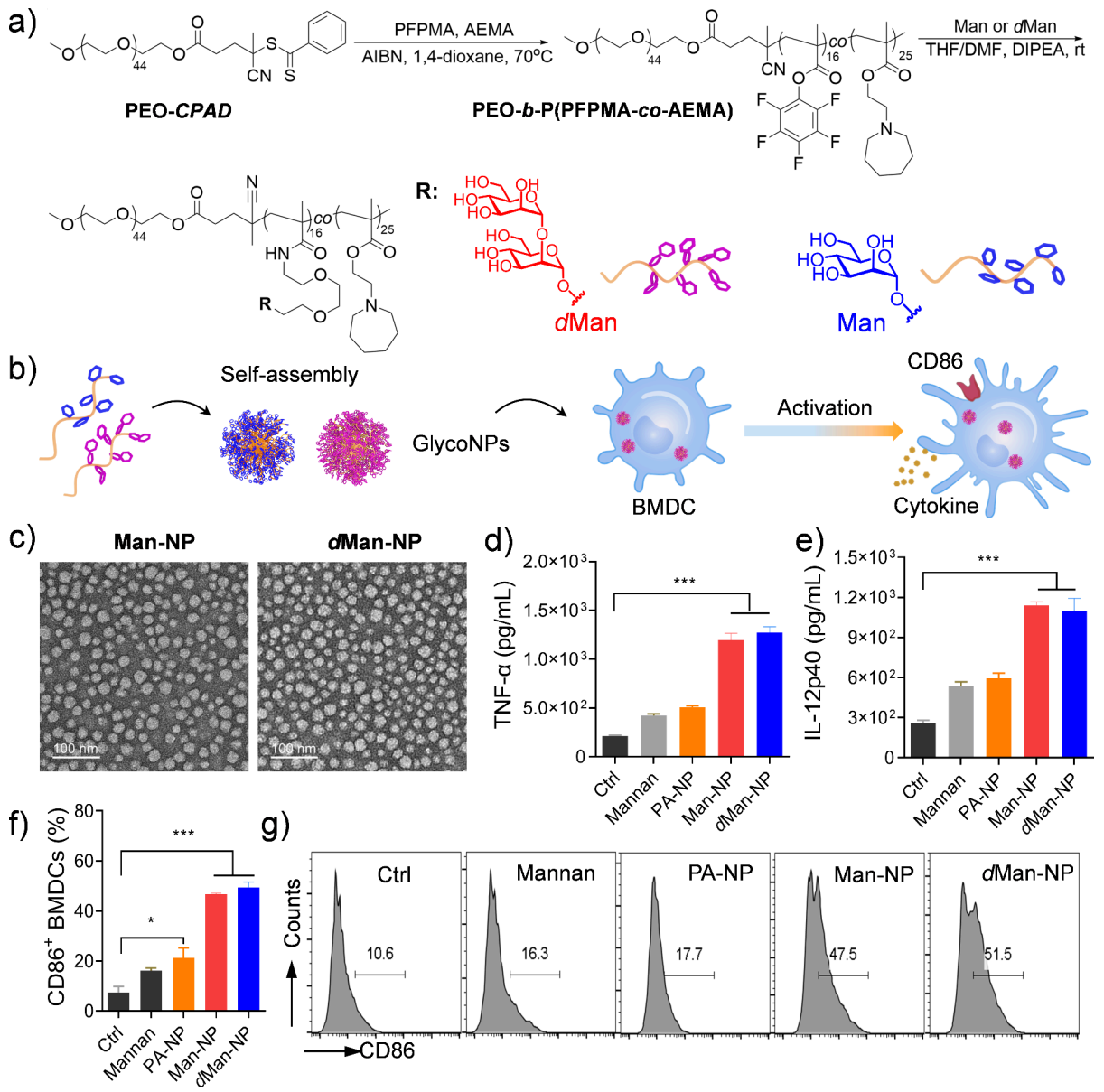

Figure 1. (a) Synthesis of amphiphilic glycopolymers. (b) Schematic illustration for BMDC activation by glyco-nanoparticles. (c) TEM images of glyco-nanoparticles. (d, e) The concentrations of TNF-α and IL-12p40 secreted by nanoparticles-treated BMDCs. (f, g) Percentages and representative flow cytometry histograms of $CD86^+$ BMDCs. Bar graphs show the mean ± SD ($n = 3$, t test or one-way ANOVA, $^*P < 0.05$; $^{**}P < 0.01$; $^{***}P < 0.001$).

https://doi.org/10.1021/acsmacrolett.5c00712
ACS Macro Lett. 2026, 15, 165−173

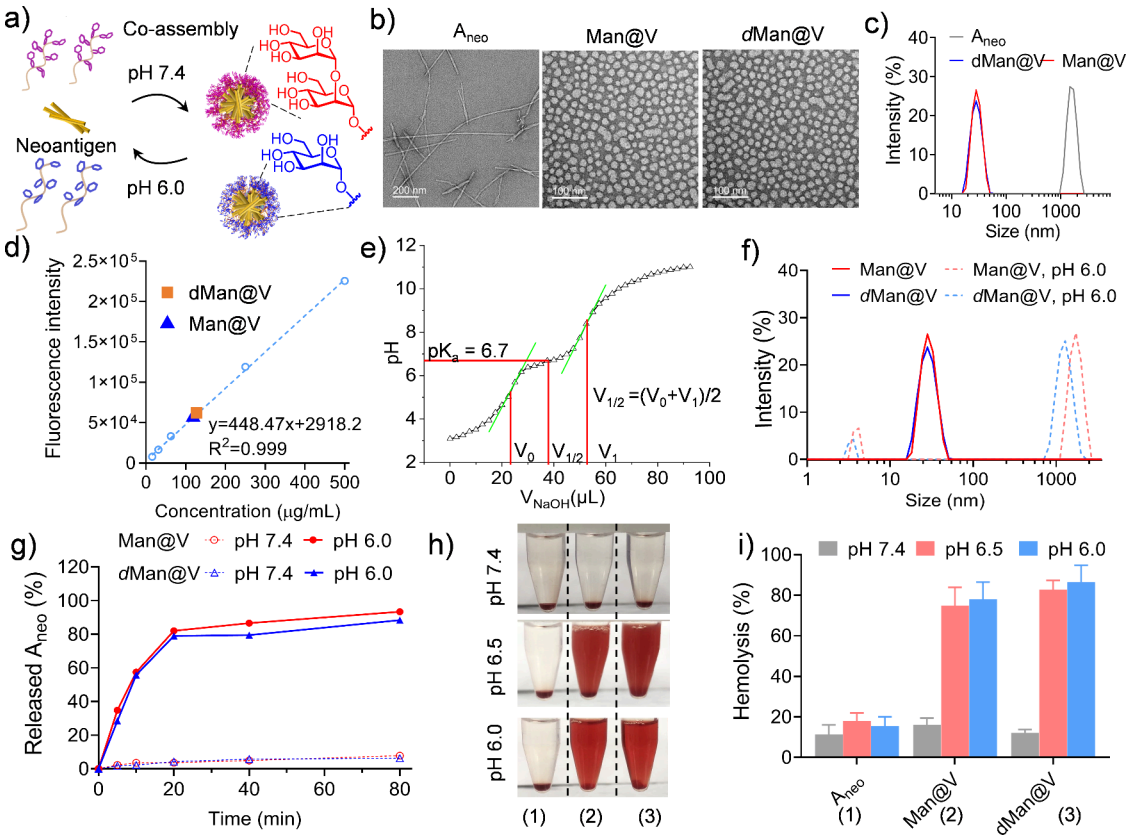

Figure 2. (a) Schematic illustration of pH-responsive antigen release by coassembled nanoparticle. (b) Morphology and (c) hydrodynamic diameter of A_{neo}, Man@V, and *d*Man@V. (d) Calibration of fluorescence intensity against concentration of FITC-neoantigen standard. (e) pK_a determination of glycopolymers with dimannopyranoside modification. (f) Size distribution of Man@V and *d*Man@V under acidic condition. (g) Release profiles of neoantigen at different pH conditions. (h) Images of erythrocytolysis. (i) Hemolysis ratios of erythrocytes at different pH conditions (n = 3).

Adpgk (A_{neo}) was selected as a model and loaded into these glyconanoparticles to form nanovaccines. These nanovaccines facilitated efficient internalization by BMDCs and promoted endosomal escape of the neoantigen via the acid-sensitive units on glycopolymers. Among them, the nanovaccine with the dimannopyranoside modification showed better effects on the delivery efficacy of neoantigen. In vitro studies indicated that neoantigen presented by MHC I pathway of BMDCs could significantly improve the proliferation and activation of cytotoxic $CD8^+$ T cells. These results highlighted the potential of glycocalyx-mimicking nanovehicles with immune-activating functions to potentiate the immunogenicity of neoantigens by improving delivery and presentation efficacy, opening a new avenue for the development of subunit vaccines and cancer immunotherapy.

Inspired by the structure of mannan, a polysaccharide composed of repetitive mannoside residues that have been employed as an immune agonist,[36−38] we synthesized natural fragment mannoside derivatives, Man and $\alpha(1\rightarrow2)$-linked *d*Man (Schemes S1−S4). Next, a methacrylate monomer containing pentafluorophenyl group (PFPMA) was prepared for coupling with the mannoside derivatives,[40] and the acid-sensitive 2-azacycloheptane-1-ethyl methacrylate (AEMA) monomer with seven-membered tertiary amines was introduced. Incorporation of PFPMA monomer and AEMA monomer into a copolymer via reversible addition−fragmentation chain transfer (RAFT) polymerization obtained poly(ethylene glycol)$_{44}$-*b*-poly(PFPMA-*co*-AEMA)$_n$ (termed as PEO-*b*-P(PFPMA-*co*-AEMA)) (Figure 1a).[41,42,46] The copolymer possessed a molecular weight of 8.2 kDa (M_w/M_n = 1.13) and comprised PFPMA segments (DP = 16) and AEMA segments (DP = 25) (Figure S12). Then, aminated monomannoside and dimannopyranoside derivatives were conjugated to the side chains of copolymers and formed glycopolymers PEO-*b*-P(Man-*co*-AEMA) and PEO-*b*-P(*d*Man-*co*-AEMA) (Figures 1a and S15−S17). The result of ^{19}F nuclear magnetic resonance (NMR) spectra showed the disappearance of the characteristic pentafluorophenyl signals at δ-149, -157, and -162 ppm, confirming that both the mannoside and dimannoside were successfully incorporated into the polymers. The obtained glycopolymers were dissolved in THF/DMF (4/1, v/v), and then slowly dropped into phosphate buffered saline (PBS) under vigorous stirring, followed by dialysis against PBS. The results of transmission electron microscopy (TEM) showed that these glycopolymers assembled into micellar nanoparticles with a diameter of about 40 nm, termed as Man-NP and *d*Man-NP, respectively (Figure 1c). Moreover, nonglycosylated copolymer also assembled into nanoparticles, named as PA-NP (Figure S19).

Furthermore, BMDCs were employed to investigate the immune activity of these glyco-nanoparticles (Figure 1b). The cytotoxicity of the assemblies was first examined by incubation with BMDCs at serial dilution concentrations for 24 h. Cell counting kit-8 (CCK8) results showed that all assemblies had no obvious cytotoxicity at concentrations of up to 100 μg/mL (Figure S20). After overnight incubation, enzyme-linked

https://doi.org/10.1021/acsmacrolett.5c00712
ACS Macro Lett. 2026, 15, 165−173

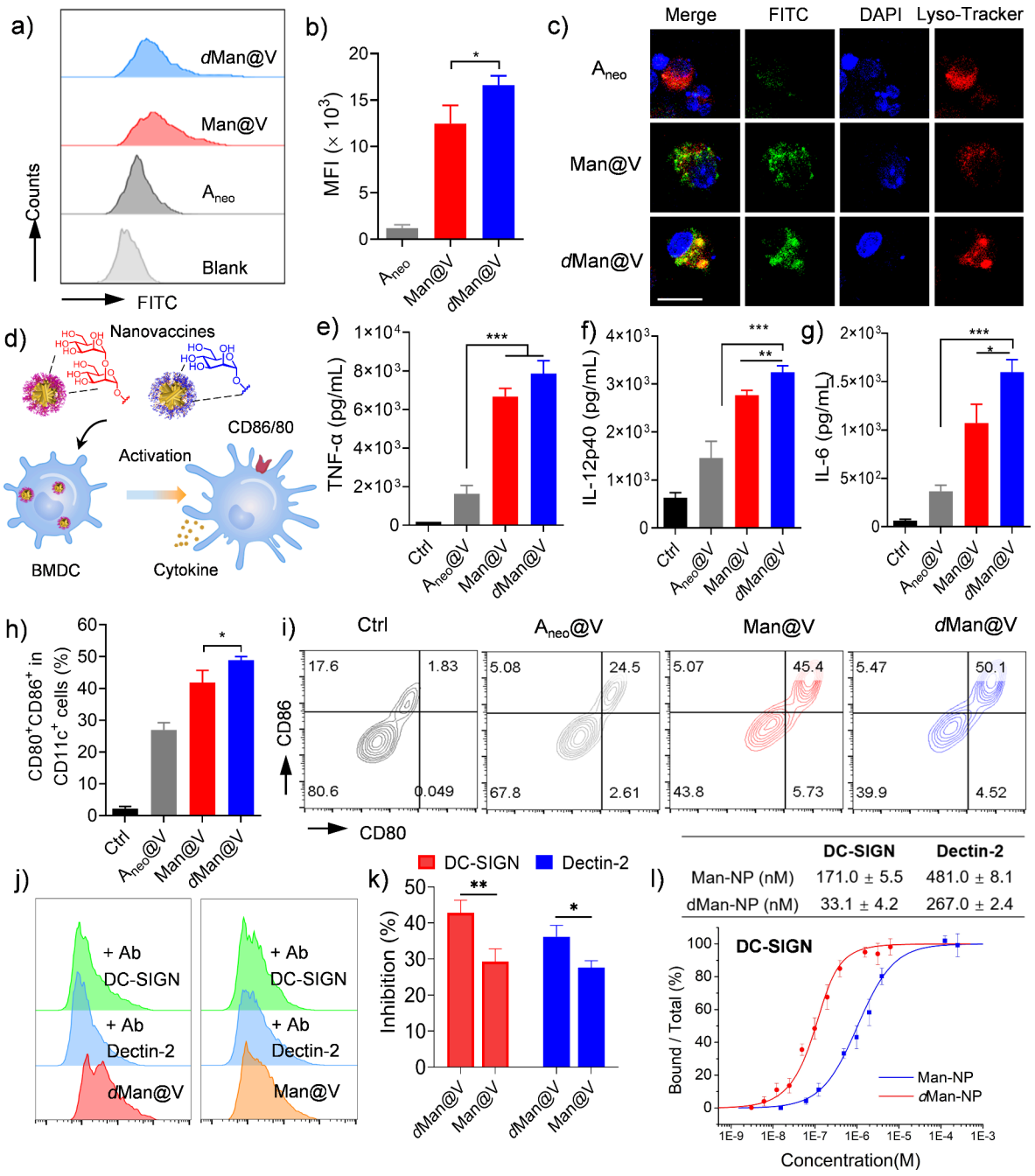

Figure 3. (a, b) Percentages and representative flow cytometry histograms of nanovaccines internalized by BMDCs. (c) Confocal imaging of BMDCs treated by nanovaccines after 6 h. The cells were costained by DAPI (blue) and Lyso-Tracker (red). (d) Illustration for the nanvaccines in activating BMDCs. (e−g) The concentrations of TNF-α, IL-12p40, and IL-6 secreted by nanoparticles-treated BMDCs. (h, i) Percentages and representative flow cytometry histograms of $CD11c^+CD80^+CD86^+$ BMDCs following various treatments. (j, k) Representative flow cytometry histograms and percentages of glyconanoparticles uptaked by BMDCs after receptor blockade. (l) Binding affinities and representative MST results of glyconanoparticles to DC-SIGN. Bar graphs show the mean ± SD (n = 3, t test or one-way ANOVA, $^*P < 0.05$; $^{**}P < 0.01$; $^{***}P < 0.001$).

immunosorbent assay (ELISA) was employed to detect the secretion of proinflammatory cytokines by BMDCs, including tumor necrosis factor α (TNF-α) and interleukin 12 (IL-12). As shown in Figure 1d, both glyconanoparticles induced a significant increase in TNF-α secretion, which was approximately 2.5-fold compared to the mannan and PA-NP groups. Consistent with TNF-α, the secretion of IL-12 also increased significantly (Figure 1e), indicating that glyconanoparticles had a strong immune-activating effect on BMDCs. The expression of CD86, a surface marker expressed on mature BMDCs was further analyzed by flow cytometry.[43] The results showed that after glyconanoparticle treatment the proportion of $CD86^+$ BMDCs increased to 51.5% (*d*Man-NP) and 47.5% (Man-NP) (Figure 1f, 1g). Together, these results indicate that glycocalyx-mimicking nanoparticles not only stimulate the secretion of proinflammatory cytokines by BMDCs but also enhance the maturation of primary BMDCs, demonstrating their ability to serve as adjuvants for active immune responses.

Encouraged by these results, the neoantigen A_{neo} (ASMTN-MELM) was selected to coassemble with these glycopolymers

https://doi.org/10.1021/acsmacrolett.5c00712
ACS Macro Lett. 2026, 15, 165−173

to generate nanovaccine. A_{neo} peptide exhibits a strong Tyndall phenomenon in aqueous solution (1 mg/mL), indicating its poor solubility and ready aggregation due to the hydrophobic amino acids. Microscopically, TEM observations showed that A_{neo} self-assembled into fibers over several micrometers (Figure 2b). Following the same process of fabricating glyconanoparticles, A_{neo} coassembled with the two glycopolymers could generate nanoparticles with similar diameters, termed as Man@V and *d*Man@V, respectively (Figure 2b). The results of Dynamic Light Scattering (DLS) further confirmed that coassembly with glycopolymers improved the hydrodynamic diameter of the neoantigens from larger aggregates to smaller nanoparticles (Figure 2c). Meanwhile, fluorescein isothiocyanate labeled A_{neo} peptides (FITC-A_{neo}) were used to evaluate the antigen encapsulation efficiency of the glycopolymers by redissolving the nanoparticles in dimethyl sulfoxide (DMSO). Based on the standard calibration curve of FITC fluorescence intensity versus antigen concentration, there was no significant difference in the peptide loading between Man@V (60.9%) and *d*Man@V (61.2%) (Figure 2d). In subsequent experiments, the content of A_{neo} was defined as the concentration of A_{neo}@V, Man@V, and *d*Man@V.

Antigen presentation by APCs occurs primarily through two pathways. One is that the internalized antigen is processed in lysosomes and loaded onto MHC II molecules for presentation to $CD4^+$ T cells, and the other is that the cytoplasmic antigen is bound to MHC I molecules and presented to $CD8^+$ T cells to induce a direct cytotoxic response.[44] Efficient cross-presentation requires the antigen to escape from endosomes (pH 5.0−6.5) into the cytosol (pH 7.0−7.4), thereby facilitating antigen release and cytoplasmic delivery.[29,44] Therefore, to further test the responsiveness of nanovaccines in different pH environments (Figure 2a), the apparent pK_a values of the glycopolymers were first determined. The results showed that both monomannoside-modified and dimannoside-modified polymers exhibited essentially identical pK_a values of approximately 6.7 (Figures 2e, S21, and S22). This indicates that the polymers could become increasingly protonated as the pH decreases. Based on this result, a pH range from 6.0 to 7.4 was selected to systematically investigate the pH-responsive behavior of the nanovaccines. After incubation of these nanovaccines under a mimic endosomal condition (pH 6.0), DLS analysis revealed the reappearance of micrometer-sized aggregates, indicating that the A_{neo} peptide was released through nanoparticle disassembly in the acidic environment (Figure 2f). The release efficiency of the peptide was further revealed by FITC-A_{neo} encapsulated nanovaccines. Fluorescence measurements showed that the encapsulated A_{neo} peptide could be released rapidly within 20 min, reaching approximately 90% release at 80 min in both Man@V and *d*Man@V (Figure 2g). These results demonstrated that the nanovaccines could be decomposed in an acidic environment and achieve effective antigen release by protonation of the AEMA fragment. Another important factor contributing to endosomal escape is the lipid membrane disruption caused by the proton sponge effect, which was further investigated by red blood cell (RBC) hemolysis assay. As shown in Figure 2h, A_{neo} peptide could not damage the RBC membrane, while Man@V and *d*Man@V triggered hemoglobin release at pH 6.5 and 6.0, indicating lipid membrane disintegration. This was further confirmed by UV−vis spectroscopy of the supernatant at characteristic hemoglobin absorption peak (540 nm; Figure 2i). These results confirmed that the acid responsiveness of the nanovaccine could promote the release of the neoantigen peptides encapsulated in the nanoparticles and disrupt the lipid membrane.

After the construction of self-assembled nanovaccines, we evaluated the cellular internalization by incubating BMDCs with free FITC-A_{neo}, Man@V, and *d*Man@V at a concentration of 30 μg/mL. Flow cytometric analysis showed that, both glyco-nanovaccines could be effectively internalized by BMDCs, but only a small amount of free A_{neo} had been taken up. Compared with that in the Man@V group, the percentage of $FITC^+$ BMDCs increased 1.4-fold after dMan@V treatment, showing that the dimannoside modification of nanoparticles could induce enhanced endocytosis in BMDCs (Figure 3a,b), as reported in our previous work.[39] Furthermore, confocal laser scanning microscopy was used to examine the intracellular distribution of the FITC-A_{neo}. As shown in Figure 3c, FITC-A_{neo} (green) was barely detectable in BMDCs treated with free A_{neo}, because its aggregation limited cellular uptake. In contrast, both Man@V and *d*Man@V enabled strong intracellular accumulation of FITC-A_{neo}, with partial colocalization with endo/lysosomes (red). Meanwhile, FITC-A_{neo} was also observed in the cytosol, suggesting that glyco-nanovaccines facilitated effective endosomal escape of the neoantigen peptide. To further assess the effects of these nanovaccines on BMDCs, A_{neo}@V (A_{neo} mixed with 200 nM CpG), Man@V, and *d*Man@V were incubated with BMDCs for 12 h (Figure 3d). The results of ELISA revealed that compared with the A_{neo}@V group, both Man@V and *d*Man@V treatments led to a significant increase in TNF-α, interleukin 6 (IL-6), and IL-12 secretion, which increased by approximately 2 to 3 times. Moreover, due to enhanced uptake capacity by the dimannoside modification, the *d*Man@V treatment led to a modest increase in these proinflammatory cytokines compared to the Man@V treatment. Immune costimulatory molecule (CD80 and CD86) expression was further confirmed by flow cytometric analysis. The proportion of $CD11c^+CD80^+CD86^+$ BMDCs treated with A_{neo}@V was 24.5%, while it increased to 50.1% and 45.4% in the Man@V and *d*Man@V groups, respectively (Figure 3h, 3i). Although A_{neo}@V contains CpG, a commonly used and potent adjuvant that activates Toll-like receptor 9 (TLR9),[45] the nanovaccines constructed by glycopolymers exhibited stronger immune activation effects than A_{neo}@V. These results demonstrated that glycopolymer nanovaccines could efficiently promote BMDCs activation as a robust immune adjuvant and deliver antigens to the cytoplasm via protonation in the endosomal environment.

The basis for the enhanced cellular internalization and BMDC stimulation by *d*Man@V over Man@V was further investigated. Since these glyconanoparticles possessed similar morphologies and sizes (Figure 1c) and mannosides typically function via C-type lectin receptors (CLRs) binding to trigger endocytosis and innate immune responses,[47] it is plausible that the difference arose from the efficiency of CLR-mediated endocytosis. Therefore, two C-type lectin receptors (Dectin-2 and DC-SIGN) binding with mannose were selected to verify this speculation. The results of antibody blockade assay showed that all C-type lectin receptor blockades could decrease the cellular uptake of nanovaccines in both *d*Man@V and Man@V groups (Figure 3j), suggesting that these glyco-nanovaccines were internalized by C-type lectin receptors of BMDCs. Meanwhile, *d*Man@V exhibited an approximately 1.5-fold enhancement in inhibitory efficacy over Man@V

https://doi.org/10.1021/acsmacrolett.5c00712
ACS Macro Lett. 2026, 15, 165−173

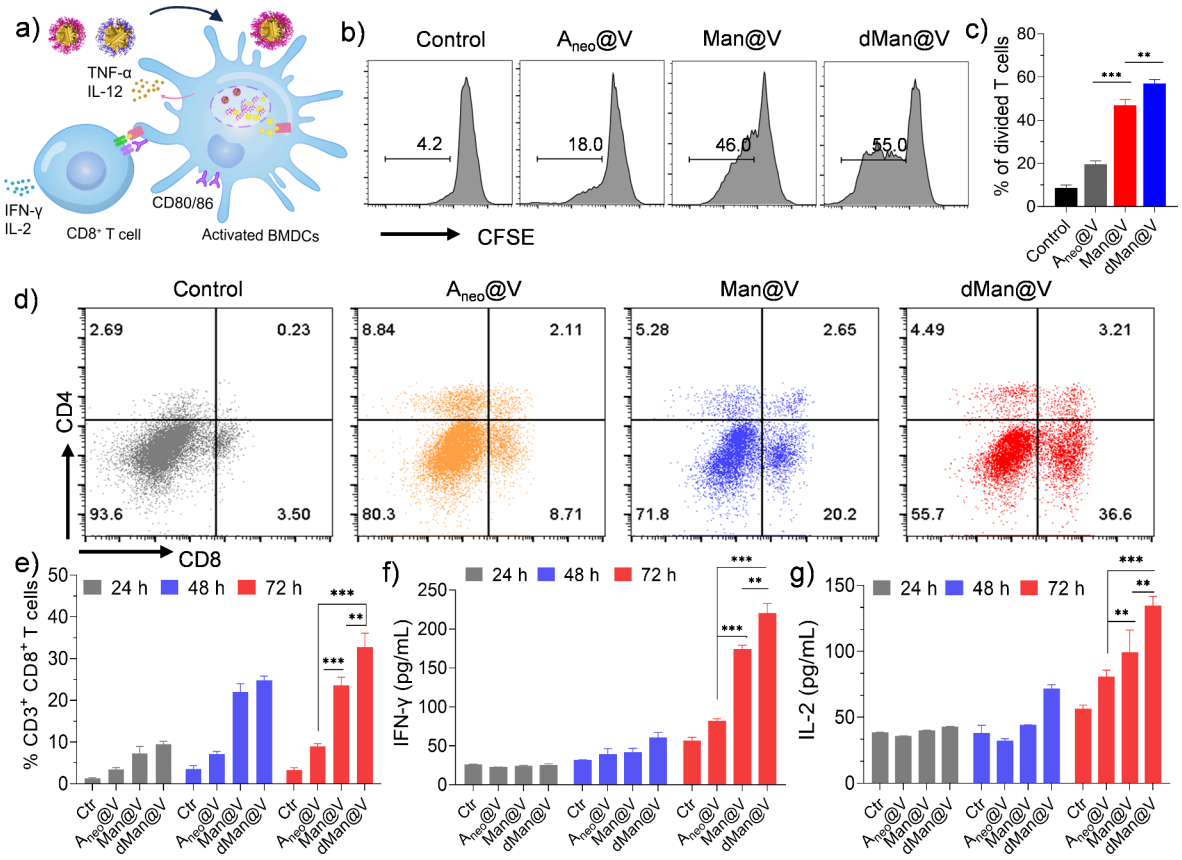

Figure 4. (a) Schematic illustration of antigen cross-presentation by BMDCs to $CD8^+$ T cells. (b) Flow cytometry profiles and (c) quantitative analysis of CFSE-labeled T cells after coculture with nanovaccine-treated BMDCs. (d, e) Representative flow cytometry plots and quantification of $CD3^+CD4^+CD8^+$ T cells after coculture with BMDCs treated by different vaccine formulations. (f) Concentrations of IFN-γ and (g) IL-2 in the supernatants of BMDC-T cell cocultures measured by ELISA (n = 3). Bar graphs show the mean ± SD (n = 3, t test or one-way ANOVA, $^*P < 0.05$; $^{**}P < 0.01$; $^{***}P < 0.001$).

(Figures 3k, S20, and S22), indicative of its superior receptor-mediated recognition. Therefore, we further determined the interaction of glyconanoparticles with recombinant Dectin-2 protein and recombinant DC-SIGN protein by microscale thermophoresis (MST) assays. The results showed that, the K_d for *d*Man-NP binding to DC-SIGN and Dectin-2 was 33.1 nM and 267.0 nM, respectively, whereas the corresponding K_d for Man-NP was 171.0 nM and 481.0 nM (Figure 3l and S23). These results demonstrated that *d*Man@V could enhance the internalization of BMDCs by increasing the affinity between saccharides and CLRs, thereby improving the efficacy of glyco-nanovaccines.

The cross-presentation capacity of nanovaccine-treated BMDCs in inducing T cell responses was subsequently evaluated (Figure 4a). Naive $CD3^+$ T cells were isolated from mouse splenocytes by magnetically activated cell sorting (MACS). Moreover, T cells were labeled with the carboxyfluorescein succinimidyl ester (CFSE) to quantitatively evaluate the ability of nanovaccine-treated BMDCs to activate T cell proliferation. After naive T cells incubated with nanovaccine-treated BMDCs for 72 h, flow cytometric analysis indicated that the T cell proliferation rate of BMDCs treated with A_{neo}@V was 18.0%, while that of BMDCs treated with Man@V and *d*Man@V was increased to 46.0% and 55.0%, respectively (Figure 4b,c). The significant improvement in T cell proliferation suggested that enhanced BMDC maturation and antigen entry into the cytoplasm by glycopolymer nanocarriers could effectively stimulate T cell responses. The phenotype of coincubated T cells was further analyzed to investigate whether endosomal escape of neoantigens could activate cytotoxic $CD8^+$ T cells via the MHC I pathway of BMDCs. The proportion of $CD8^+$ T cells showed a time-dependent increase in all treatments (Figure 4e). Quantitative analysis of the T cell subtypes at 72 h showed that, Man@V- and *d*Man@V-treated BMDCs induced a large number of $CD3^+CD8^+$ cytotoxic T lymphocytes, accounting for 20.2% and 36.6% respectively (Figure 4d,e), which were significantly higher than those of A_{neo}@V-treated BMDCs (8.71%). This result indicated that most of the A_{neo} peptides that escaped lysosomes through nanocarrier-assisted delivery were processed and presented via the MHC I pathway, demonstrating the effectiveness of acid-responsive glycocalyx-mimicking nanovehicles. The proinflammatory cytokines secreted by T cells, including interferon-γ (IFN-γ) and interleukin 2 (IL-2), were further quantitatively measured by ELISA. The time-dependent results showed that Man@V- and *d*Man@V-treated BMDCs induced significantly enhanced IFN-γ and IL-2 production by T cells, compared with A_{neo}@V (Figure 4e,f). Together, these results confirmed that glyco-nanovaccines enable a fraction of the delivered antigen to escape endosomal compartments and enter the cytosol for cross-presentation by APCs, thereby promoting T cell proliferation and differentiation.

https://doi.org/10.1021/acsmacrolett.5c00712
ACS Macro Lett. 2026, 15, 165−173

In summary, this work highlights a glycopolymer-based nanocarrier system with inherent immune-activating capabilities that enhances the immunogenicity of neoantigens by improving solubility and endocytic efficacy. By incorporation of acid-sensitive units, these nanovaccines enable efficient endosomal escape and facilitate antigen cross-presentation by APCs, resulting in robust T cell proliferation and differentiation. This work represents a pioneering effort to utilize artificial glycocalyx-inspired structures as agonists for peptide vaccine construction in the absence of other potent activators, demonstrating the potential of synthetic glycopolymers in activating immune cells and potentiating specific cytotoxic T cell responses. Moreover, this work suggests that the glycocalyx-inspired architectures that enable better cargo functions could serve as bioactive encapsulation nanoplatforms, with promising applications in biomaterials and nanomedicine.

■ ASSOCIATED CONTENT

Supporting Information

The Supporting Information is available free of charge at https://pubs.acs.org/doi/10.1021/acsmacrolett.5c00712.

Experimental materials and characterization; Synthetic procedures; Experimental methods; Details of synthesis and characterization of the glycopolymers (PDF)

■ AUTHOR INFORMATION

Corresponding Author

Long Li − *The State Key Laboratory of Molecular Engineering of Polymers and Department of Macromolecular Science, Fudan University, Shanghai 200433, China*; Email: lilong@fudan.edu.cn

Authors

Yiwei Shi − *The State Key Laboratory of Molecular Engineering of Polymers and Department of Macromolecular Science, Fudan University, Shanghai 200433, China*

Xuyang Xu − *The State Key Laboratory of Molecular Engineering of Polymers and Department of Macromolecular Science, Fudan University, Shanghai 200433, China*

Xiaomei Liu − *The State Key Laboratory of Molecular Engineering of Polymers and Department of Macromolecular Science, Fudan University, Shanghai 200433, China*

Xin Liang − *The State Key Laboratory of Molecular Engineering of Polymers and Department of Macromolecular Science, Fudan University, Shanghai 200433, China*

Xiangyun Xu − *The State Key Laboratory of Molecular Engineering of Polymers and Department of Macromolecular Science, Fudan University, Shanghai 200433, China*

Guosong Chen − *The State Key Laboratory of Molecular Engineering of Polymers and Department of Macromolecular Science, Fudan University, Shanghai 200433, China*; orcid.org/0000-0001-7089-911X

Complete contact information is available at: https://pubs.acs.org/10.1021/acsmacrolett.5c00712

Author Contributions

CRediT: **Yiwei Shi** conceptualization, data curation, formal analysis, methodology, writing - original draft; **Xuyang Xu** data curation, formal analysis, investigation, methodology; **Xiaomei Liu** data curation, formal analysis; **Xin Liang** data curation; **Xiangyun Xu** data curation, formal analysis; **Long Li** funding acquisition, investigation, project administration, supervision, writing - review & editing; **Guosong Chen** conceptualization, funding acquisition, supervision, writing - review & editing.

Notes

The authors declare no competing financial interest.

■ ACKNOWLEDGMENTS

G.C. and L.L. thank NSFC/China (52403179, 52125303, 92356305, and 22431002), the National Key Research and Development Program of China (2023YFA0915300), and Innovation Program of Shanghai Municipal Education Commission (2023ZKZD02) for financial support.

■ REFERENCES

(1) Malonis, R. J.; Lai, J. R.; Vergnolle, O. Peptide-Based Vaccines: Current Progress and Future Challenges. *Chem. Rev.* **2020**, *120* (6), 3210−3229.

(2) Hu, Z.; Ott, P. A.; Wu, C. J. Towards personalized, tumour-specific, therapeutic vaccines for cancer. *Nat. Rev. Immunol.* **2018**, *18* (3), 168−182.

(3) Liu, T. F.; Yao, W. Y.; Sun, W. Y.; Yuan, Y. H.; Liu, C.; Liu, X. H.; Wang, X. M.; Jiang, H. Components, Formulations, Deliveries, and Combinations of Tumor Vaccines. *ACS Nano* **2024**, *18* (29), 18801−18833.

(4) Yang, J.; Zhu, Y. X.; Chen, Z. X.; Tian, Z. Y.; Lin, H.; Shi, J. L. Montmorillonite-Based Oral Vaccine for Colorectal Cancer Immunotherapy through Mucosal Immune Activation. *J. Am. Chem. Soc.* **2025**, *147* (24), 21170−21183.

(5) Zou, Y. Y.; Lyu, L.; Xie, Y. T.; Yan, S. Q.; Zhao, Y.; Chen, W. S.; Liu, Y. N.; Zhao, Y. L. Active Chemical Messenger-Driven Immune Activation via Electrochemical Patch for Tumor Vaccination. *ACS Nano* **2025**, *19* (24), 22424−22441.

(6) Zhao, Y.; Baldin, A. V.; Isayev, O.; Werner, J.; Zamyatnin, A. A.; Bazhin, A. V. Cancer Vaccines: Antigen Selection Strategy. *Vaccines* **2021**, *9* (2), 85−115.

(7) Ni, Q. Q.; Zhang, F. W.; Liu, Y. J.; Wang, Z. T.; Yu, G. C.; Liang, B.; Niu, G.; Su, T.; Zhu, G. Z.; Lu, G. M.; Zhang, L. J.; Chen, X. Y. A bi-adjuvant nanovaccine that potentiates immunogenicity of neoantigen for combination immunotherapy of colorectal cancer. *Sci. Adv.* **2020**, *6* (12), eaaw6071.

(8) Repáraz, D.; Ruiz, M.; Llopiz, D.; Silva, L.; Vercher, E.; Aparicio, B.; Egea, J.; Tamayo-Uria, I.; Hervás-Stubbs, S.; García-Balduz, J.; Castro, C.; Iñarrairaegui, M.; Tagliamonte, M.; Mauriello, A.; Cavalluzzo, B.; Buonaguro, L.; Rohrer, C.; Heim, K.; Tauber, C.; Hofmann, M.; Thimme, R.; Sangro, B.; Sarobe, P. Neoantigens as potential vaccines in hepatocellular carcinoma. *J. Immunother. Cancer* **2022**, *10* (2), No. e003978.

(9) Wei, Z. T.; Zhou, C.; Zhang, Z. B.; Guan, M.; Zhang, C.; Liu, Z. M.; Liu, Q. The Landscape of Tumor Fusion Neoantigens: A Pan-Cancer Analysis. *Iscience* **2019**, *21*, 249.

(10) Chen, X. T.; Lei, L.; Yan, J. Y.; Wang, X. Z.; Li, L.; Liu, Q.; Wang, Y.; Chen, T. R.; Shao, J.; Yu, L. X.; Li, Z. J.; Zhu, L. J.; Wang, L. F.; Liu, B. R. Bifunctional Phage Particles Augment CD40 Activation and Enhance Lymph Node-Targeted Delivery of Personalized Neoantigen Vaccines. *ACS Nano* **2025**, *19* (7), 6955−6976.

(11) Awad, M. M.; Govindan, R.; Balogh, K. N.; Spigel, D. R.; Garon, E. B.; Bushway, M. E.; Poran, A.; Sheen, J. H.; Kohler, V.; Esaulova, E.; Srouji, J.; Ramesh, S.; Vyasamneni, R.; Karki, B.; Sciuto, T. E.; Sethi, H.; Dong, J. Z.; Moles, M. A.; Manson, K.; Rooney, M. S.; Khondker, Z. S.; DeMario, M.; Gaynor, R. B.; Srinivasan, L. Personalized neoantigen vaccine NEO-PV-01 with chemotherapy and anti-PD-1 as first-line treatment for non-squamous non-small cell lung cancer. *Cancer Cell* **2022**, *40* (9), 1010.

(12) Liu, H. P.; Moynihan, K. D.; Zheng, Y. R.; Szeto, G. L.; Li, A. V.; Huang, B.; Van Egeren, D. S.; Park, C.; Irvine, D. J. Structure-

based programming of lymph-node targeting in molecular vaccines. *Nature* **2014**, *507* (7493), 519.
(13) Mehta, N. K.; Pradhan, R.; Soleimany, A. P.; Moynihan, K. D.; Rothschilds, A. M.; Momin, N.; Rakhra, K.; Mata-Fink, J.; Bhatia, S. N.; Wittrup, K. D.; Irvine, D. J. Pharmacokinetic tuning of protein-antigen fusions enhances the immunogenicity of T-cell vaccines. *Nat. Biomed. Eng.* **2020**, *4* (6), 636−648.
(14) Cui, C.; Chakraborty, K.; Tang, X. A.; Schoenfelt, K. Q.; Hoffman, A.; Blank, A.; McBeth, B.; Pulliam, N.; Reardon, C. A.; Kulkarni, S. A.; Vaisar, T.; Ballabio, A.; Krishnan, Y.; Becker, L. A lysosome-targeted DNA nanodevice selectively targets macrophages to attenuate tumours. *Nat. Nanotechnol.* **2021**, *16* (12), 1394−1402.
(15) Buhrman, J. D.; Slansky, J. E. Improving T cell responses to modified peptides in tumor vaccines. *Immunol. Res.* **2013**, *55* (1−3), 34−47.
(16) Bachelder, E. M.; Pino, E. N.; Ainslie, K. M. Acetalated Dextran: A Tunable and Acid-Labile Biopolymer with Facile Synthesis and a Range of Applications. *Chem. Rev.* **2017**, *117* (3), 1915−1926.
(17) Bertozzi, C. R.; Kiessling, L. L. Chemical glycobiology. *Science* **2001**, *291* (5512), 2357−2364.
(18) Su, L.; Feng, Y. L.; Wei, K. C.; Xu, X. Y.; Liu, R. Y.; Chen, G. S. Carbohydrate-Based Macromolecular Biomaterials. *Chem. Rev.* **2021**, *121* (18), 10950−11029.
(19) Kuo, J. C. H.; Gandhi, J. G.; Zia, R. N.; Paszek, M. J. Physical biology of the cancer cell glycocalyx. *Nat. Phys.* **2018**, *14* (7), 658−669.
(20) Huang, M. L.; Smith, R. A. A.; Trieger, G. W.; Godula, K. Glycocalyx Remodeling with Proteoglycan Mimetics Promotes Neural Specification in Embryonic Stem Cells. *J. Am. Chem. Soc.* **2014**, *136* (30), 10565−10568.
(21) Li, L.; Chen, G. S. Precise Assembly of Proteins and Carbohydrates for Next-Generation Biomaterials. *J. Am. Chem. Soc.* **2022**, *144* (36), 16232−16251.
(22) Whang, C. H.; Hong, J.; Kim, D.; Ryu, H.; Jung, W.; Son, Y.; Keum, H.; Kim, J.; Shin, H.; Moon, E.; Noh, I.; Lee, H. S.; Jon, S. Systematic Screening and Therapeutic Evaluation of Glyconanoparticles with Differential Cancer Affinities for Targeted Cancer Therapy. *Adv. Mater.* **2022**, *34* (30), e2203993.
(23) Su, L.; Zhang, W. Y.; Wu, X. L.; Zhang, Y. F.; Chen, X.; Liu, G. W.; Chen, G. S.; Jiang, M. Glycocalyx-Mimicking Nanoparticles for Stimulation and Polarization of Macrophages via Specific Interactions. *Small* **2015**, *11* (33), 4191−4200.
(24) Qi, W. J.; Zhang, Y. F.; Wang, J.; Tao, G. Q.; Wu, L. B.; Kochovski, Z.; Gao, H. J.; Chen, G. S.; Jiang, M. Deprotection-Induced Morphology Transition and Immunoactivation of Glycovesicles: A Strategy of Smart Delivery Polymersomes. *J. Am. Chem. Soc.* **2018**, *140* (28), 8851−8857.
(25) Xiao, Q.; Ludwig, A. K.; Romanò, C.; Buzzacchera, I.; Sherman, S. E.; Vetro, M.; Vértesy, S.; Kaltner, H.; Reed, E. H.; Möller, M.; Wilson, C. J.; Hammer, D. A.; Oscarson, S.; Klein, M. L.; Gabius, H. J.; Percec, V. Exploring functional pairing between surface glycoconjugates and human galectins using programmable glycodendrimersomes. *Proc. Natl. Acad. Sci. U. S. A.* **2018**, *115* (11), E2509−E2518.
(26) Wu, L. B.; Zhang, Y. F.; Li, Z.; Yang, G.; Kochovski, Z.; Chen, G. S.; Jiang, M. ″Sweet″ Architecture-Dependent Uptake of Glycocalyx-Mimicking Nanoparticles Based on Biodegradable Aliphatic Polyesters by Macrophages. *J. Am. Chem. Soc.* **2017**, *139* (41), 14684−14692.
(27) Lin, Y. N.; Su, L.; Smolen, J.; Li, R. C.; Song, Y.; Wang, H.; Dong, M.; Wooley, K. L. Co-assembly of sugar-based amphiphilic block polymers to achieve nanoparticles with tunable morphology, size, surface charge, and acid-responsive behavior. *Mater. Chem. Front.* **2018**, *2* (12), 2230−2238.
(28) Miura, Y.; Hoshino, Y.; Seto, H. Glycopolymer Nanobiotechnology. *Chem. Rev.* **2016**, *116* (4), 1673−1692.
(29) De Mel, J.; Hossain, M.; Shofolawe-Bakare, O.; Mohammad, S. A.; Rasmussen, E.; Milloy, K.; Shields, M.; Roth, E. W.; Arora, K.; Cueto, R.; Tang, S. C.; Wilson, J. T.; Smith, A. E.; Werfel, T. A. Dual-Responsive Glycopolymers for Intracellular Codelivery of Antigen and Lipophilic Adjuvants. *Mol. Pharmaceutics* **2022**, *19* (12), 4705−4716.
(30) Zhu, Z. C.; Heng, X. Y.; Shan, F. J.; Yang, H.; Wang, Y. C.; Zhang, H. Y.; Chen, G. J.; Chen, H. Customizable Glycopolymers as Adjuvants for Cancer Immunotherapy: From Branching Degree Optimization to Cell Surface Engineering. *Biomacromolecules* **2024**, *25* (12), 7975−7984.
(31) Yamazoe, S.; Sadanala, K.; Zhang, Q.; Rajpal, A.; Sproul, T.; Strop, P.; Broz, M. Design and Characterization of an Anti-Clec9a Antibody Armed with CpG Oligonucleotides To Enable Targeted Delivery of Adjuvant to Cross-Presenting Dendritic Cells. *ACS Chem. Biol.* **2025**, *20* (9), 2180−2190.
(32) Lin, Y. H.; Chen, C. W.; Chen, M. Y.; Xu, L.; Tian, X. J.; Cheung, S. H.; Wu, Y. L.; Siriwon, N.; Wu, S. H.; Mou, K. Y. The Bacterial Outer Membrane Vesicle-Cloaked Immunostimulatory Nanoplatform Reinvigorates T Cell Function and Reprograms Tumor Immunity. *ACS Nano* **2025**, *19* (21), 19866−19889.
(33) Zou, Y.; Li, S. S.; Li, Y. D.; Zhang, D. Y.; Zheng, M.; Shi, B. Y. Glioblastoma Cell Derived Exosomes as a Potent Vaccine Platform Targeting Primary Brain Cancers and Brain Metastases. *ACS Nano* **2025**, *19* (18), 17309−17322.
(34) Noble, J.; Zimmerman, A.; Fromen, C. A. Potent Immune Stimulation from Nanoparticle Carriers Relies on the Interplay of Adjuvant Surface Density and Adjuvant Mass Distribution. *ACS Biomater. Sci. Eng.* **2017**, *3* (4), 560−571.
(35) Yin, W. Z.; Deng, B. H.; Xu, Z. Y.; Wang, H. Y.; Ma, F.; Zhou, M. X.; Lu, Y.; Zhang, J. Q. Formulation and Evaluation of Lipidized Imiquimod as an Effective Adjuvant. *ACS Infect. Dis.* **2023**, *9* (2), 378−387.
(36) Mu, R. Y.; Dong, L.; Wang, C. M. Carbohydrates as putative pattern recognition receptor agonists in vaccine development. *Trends Immunol.* **2023**, *44* (10), 845−857.
(37) Borriello, F.; Poli, V.; Shrock, E.; Spreafico, R.; Liu, X.; Pishesha, N.; Carpenet, C.; Chou, J.; Di Gioia, M.; McGrath, M. E.; Dillen, C. A.; Barrett, N. A.; Lacanfora, L.; Franco, M. E.; Marongiu, L.; Iwakura, Y.; Pucci, F.; Kruppa, M. D.; Ma, Z. C.; Lowman, D. W.; Ensley, H. E.; Nanishi, E.; Saito, Y.; O'Meara, T. R.; Seo, H. S.; Dhe-Paganon, S.; Dowling, D. J.; Frieman, M.; Elledge, S. J.; Levy, O.; Irvine, D. J.; Ploegh, H. L.; Williams, D. L.; Zanoni, I. An adjuvant strategy enabled by modulation of the physical properties of microbial ligands expands antigen immunogenicity. *Cell* **2022**, *185* (4), 614.
(38) Faustino, M.; Durao, J.; Pereira, C. F.; Pintado, M. E.; Carvalho, A. P. Mannans and mannan oligosaccharides (MOS) from Saccharomyces cerevisiae-A sustainable source of functional ingredients. *Carbohydr. Polym.* **2021**, *272* (15), No. 118467.
(39) Yin, L.; Xu, X. Y.; Shi, Y. W.; Xu, X. Y.; Liu, X. M.; An, J. Y.; Du, Q. Q. G.; Li, L.; Chen, G. S. Synergistic Programming of Macrophages by Hybrid Glycocalyx-Inspired Nanoparticles for Adoptive Cell Therapy. *J. Am. Chem. Soc.* **2025**, *147* (42), 38838−38850.
(40) Zhao, Y.; Zhang, Y. F.; Wang, C. C.; Chen, G. S.; Jiang, M. Role of Protecting Groups in Synthesis and Self-Assembly of Glycopolymers. *Biomacromolecules* **2017**, *18* (2), 568−575.
(41) Zhou, K. J.; Wang, Y. G.; Huang, X. N.; Luby-Phelps, K.; Sumer, B. D.; Gao, J. M. Tunable, Ultrasensitive pH-Responsive Nanoparticles Targeting Specific Endocytic Organelles in Living Cells. *Angew. Chem., Int. Ed.* **2011**, *50* (27), 6109−6114.
(42) Rieger, J.; Stoffelbach, F.; Bui, C.; Alaimo, D.; Jérôme, C.; Charleux, B. Amphiphilic poly(ethylene oxide) macromolecular RAFT agent as a stabilizer and control agent in ab initio batch emulsion polymerization. *Macromolecules* **2008**, *41* (12), 4065−4068.
(43) Kennedy, A.; Waters, E.; Rowshanravan, B.; Hinze, C.; Williams, C.; Janman, D.; Fox, T. A.; Booth, C.; Pesenacker, A. M.; Halliday, N.; Soskic, B.; Kaur, S.; Qureshi, O. S.; Morris, E. C.; Ikemizu, S.; Paluch, C.; Huo, J. D.; Davis, S. J.; Boucrot, E.; Walker, L. S. K.; Sansom, D. M. Differences in CD80 and CD86 transendocytosis reveal CD86 as a key target for CTLA-4 immune regulation. *Nat. Immunol.* **2022**, *23* (9), 1365−1378.

https://doi.org/10.1021/acsmacrolett.5c00712
ACS Macro Lett. 2026, 15, 165−173

(44) Li, H. M.; Nelson, C. E.; Evans, B. C.; Duvall, C. L. Delivery of Intracellular-Acting Biologics in Pro-Apoptotic Therapies. *Curr. Pharm. Des.* **2011**, *17* (3), 293−319.
(45) Lucas, S. N.; Archer, P. A.; Yoon, T. H.; Manspeaker, M. P.; Levitan, M.; Kim, J.; Thomas, S. N. Thermosensitive Hydrogel Sustaining the Release of Lymph-Draining Oligonucleotide Adjuvant Polyplex Micelles Improves Systemic Cancer Immunotherapy. *ACS Nano* **2025**, *19* (23), 21775−21791.
(46) Zhao, Y.; Zhang, Y. F.; Wang, C. C.; Chen, G. S.; Jiang, M. Role of Protecting Groups in Synthesis and Self-Assembly of Glycopolymers. *Biomacromolecules* **2017**, *18* (2), 568−575.
(47) Wawrzinek, R.; Wamhoff, E. C.; Lefebre, J.; Rentzsch, M.; Bachem, G.; Domeniconi, G.; Schulze, J.; Fuchsberger, F. F.; Zhang, H. X.; Modenutti, C.; Schnirch, L.; Marti, M. A.; Schwardt, O.; Bräutigam, M.; Guberman, M.; Hauck, D.; Seeberger, P. H.; Seitz, O.; Titz, A.; Ernst, B.; Rademacher, C. A Remote Secondary Binding Pocket Promotes Heteromultivalent Targeting of DC-SIGN. *J. Am. Chem. Soc.* **2021**, *143* (45), 18977−18988.

https://doi.org/10.1021/acsmacrolett.5c00712
ACS Macro Lett. 2026, 15, 165−173